

Effect of Compressive Loads on the Air-Permeability  $kT$  of ConcreteR.J. Torrent<sup>2\*</sup>, M. Paderi<sup>1</sup> and C. Paglia<sup>1</sup>

<sup>1</sup>SUPSI, Univ. of Southern Switzerland, CH-6850 Mendrisio, Switzerland.

<sup>2</sup>Materials Advanced Services Ltd., CH-6877 Coldrerio, Switzerland, C1425ABV

**\*Correspondence authors**

**C. Paglia,**  
SUPSI,  
Univ. of Southern Switzerland,  
CH-6850 Mendrisio,  
Switzerland.

**R.J. Torrent,**  
Materials Advanced Services Ltd.,  
CH-6877 Coldrerio, Switzerland,  
C1425ABV Buenos Aires,  
Argentina.

Submitted : 11 Apr 2023 ; Published : 24 May 2023

**Citation :** Torrent R. et al (2023). Effect of Compressive Loads on the Air-Permeability  $kT$  of Concrete. *J mate poly sci*, 3(2): 1-7.

**Abstract**

Since long it has been claimed that the departure from linearity of the  $\sigma$ - $\varepsilon$  relation for concrete, up to failure under compression, is the result of cracks formation, first along the aggregate-paste interface, which later bridge the aggregates until, at around 75-80% of the maximum load (critical stress level), the matrix cracks become unstable, such that if that load is sustained, fracture will happen after a certain period (due to tertiary creep). This fact has been verified measuring volumetric strains, acoustic emission and ultrasound. The presence, growth and opening of such cracks must have an effect on the permeability of concrete, which was confirmed by water- and gas-permeability tests. The phenomenon was also studied applying a standard NDT method for air-permeability, based on a double-chamber vacuum cell, same as applied in the here reported research. This paper reports results of air-permeability  $kT$  of concrete cubes and half-cubes subjected to the following loading conditions: unloaded, sustained loads of 30, 60 and 90% of the ultimate load (measuring  $kT$  under the applied static load and the residual value after removing it) and dynamically during a test with monotonically increasing load till failure. The results indicate that a certain degree of damage, reflected in an increase of  $kT$ , is noticeably already at a 30% load level, which increases with the level of applied load. The dynamic  $kT$  tests were somewhat erratic, possibly, depending on whether the damage happened near or away from the surface where  $kT$  was measured.

**Introduction**

Since long it has been claimed that the departure from linearity of the  $\sigma$ - $\varepsilon$  relation for concrete, up to failure under compressive load, is the result of cracks formation (Hsu et al, 1963; Shah & Slate, 1968; Newman & Newman, 1971).

In a test under monotonically increasing compressive load, initially, up to  $\approx 30\%$  of the ultimate load, the  $\sigma$ - $\varepsilon$  relation is quasi-linear (this is the region where, typically the elastic modulus is measured) and the behaviour of the material is quasi-elastic; i.e., if the specimen is unloaded from this load level, no noticeable residual deformations are measured. At higher levels of load, cracks begin to develop and grow in the material, first along the aggregate-paste interface, later bridging the aggregates until, at around 75-80% of the maximum load (critical stress level), the matrix cracks become unstable, such that if that load is sustained, fracture will happen after a certain period (due to tertiary creep) (Rüsch, 1960). The predominant orientation of these cracks is along vertical planes, which theoretically, are subjected to a null stress. But this is on average; due to the strong heterogeneity of the material, tensile

stresses can develop locally, especially at the aggregate-paste interface which can initiate the cracking process. This was established already in the 50's by photoelasticity analysis (Dantu, 1958).

The generation and propagation of cracks was made evident through microscopy observation of slices of concrete, obtained from specimens that had been subjected to increasing levels of compressive load (Hsu et al, 1963). Another evidence of the crack formation and propagation was provided through acoustic emission, measured under a monotonically increasing load (Mlakar et al., 1984). Another evidence of crack opening was provided by the measurement of volumetric strains of a concrete specimen under uniaxial compression (by measuring longitudinal and transverse deformations with strain-gauges). In theory, as the Poisson coefficient of concrete is  $\approx 0.20$ , the volumetric deformation of concrete  $\varepsilon_v$  under uniaxial compression, should lead to a contraction of the order of 0.6 of the longitudinal compressive strain (Newman & Newman, 1971). This performance is observed up to the critical load,

beyond which a reverse in the behaviour happens, with the volumetric strain now starting to increase rapidly, due to a huge increase in the tensile transverse deformations due to the opening of the cracks.

All these pioneer investigations were made at the time (1950-1970) when the fundamentals of the mechanical behaviour of concrete were established in view of developing sound models for the structural design of reinforced concrete structures. Since the application of a compressive load leads to the appearance and propagation of cracks, an increase of the permeability of the material with the level of applied loads is to be expected. However, permeability test methods for concrete began to be established only around 1990. A literature review of the effect of loads on the permeability of concrete to liquids, gases and chlorides was published by (Hoseini et al, 2009) and, more recently, by (Torrent et al, 2022).

There is a certain agreement in that, at relatively low level of compressive stresses (up to about 50% of the compressive strength), the permeability of concrete slightly decreases. This is attributed to the effect of consolidation and closure of micro-cracks (mostly originated by shrinkage) that already exist in unloaded concrete [Shah & Slate, 1968]. Beyond 50% of the maximum load, the permeability starts to slightly increase, until the critical stress level is reached ( $\approx 75\%$ – $80\%$  of the compressive strength), after which a very sharp increase in permeability is observed. Figure 1 presents results reported by (Li, 2016), originated by Meziani and Skoczylas (1999) and Banthia and Barghava (2007), that confirm that behaviour.

Besides these fundamental aspects of the problems, there is a practical one. The double-chamber vacuum cell method, standardized in Switzerland [SIA 262/1, 2019], Japan (NDIS 3436-2, 2020) and Argentina (IRAM 1892, 2022), aimed at measuring the coefficient of air-permeability  $kT$ , can be applied on site on structural members. It is therefore important to know whether loads applied to the elements may affect the results of the test.

In previous investigations, concrete cubes were loaded up to a certain level of stress, measuring the coefficient of air-permeability  $kT$  of the cubes, under a sustained load. (Paulík & Hudoba, 2009) found, for plain concrete, that the  $kT$  value under a stress of 30% of the compressive strength was the same as for the unloaded cube, recording a 10-fold increase for tests performed at 60% of the compressive strength. (Van der Merwe, 2019) tested cubes of six different compositions, unloaded and loaded at stresses up to 50% of the compressive strength. He proved that there is no statistically significant effect of compressive load on the air-permeability of concrete within load levels expected during typical service conditions, and can therefore be ignored in practice.

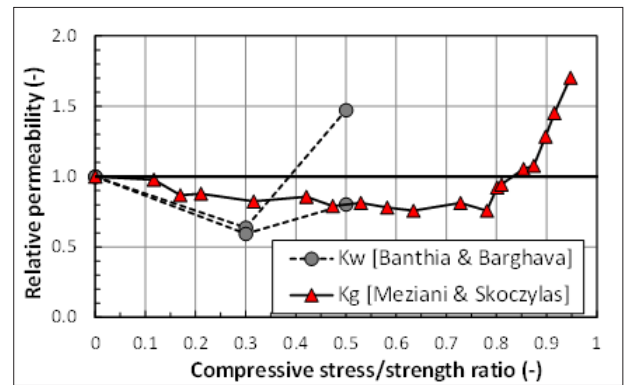


**Figure 1:** Effect of applied compressive stress on the permeability of concrete to gas  $K_g$  and water  $K_w$ ; data from (Meziani & Skoczylas, 1999; Banthia & Barghava, 2007) apud (Li, 2016).

In both investigations described above, the values of  $kT$  were recorded loading the cubes up to a certain level and measuring the air-permeability under a constant sustained load.

It was considered of interest to investigate the changes in  $kT$  experienced by specimens under monotonically increasing loads until failure. The object of this paper is to present preliminary results of measurements of the coefficient of air-permeability  $kT$ , of a single concrete mix, obtained under four different loading conditions:

- Unloaded cubes, before applying any load
- Under sustained compressive stresses of 30, 60 and 90% of the compressive strength
- The residual value after removing the load of cubes tested as described in b.
- Under monotonically increasing loads until failure

### Experimental Methodology Concrete Characteristics and Specimens

Seventeen 150 mm cubes were cast from a single batch of a concrete mix of the composition shown in Table 1. The cubes were moist-cured during 140 days, age at which some cubes were tested for compressive strength, yielding a mean value  $f'_{cm} = 45.0$  MPa.

Constituent	Cement	Water	Aggregates	Plasticizer
kg/m <sup>3</sup>	320	160	1960	2.9

**Table 1:** Composition of the concrete mix investigated

### Air-Permeability Test Method

The test method consists in placing a vacuum cell composed of two concentric chambers in contact with the concrete surface and creating a vacuum of  $\approx 30$  mbar in both chambers by means of a vacuum pump. After 60 seconds, the central (test) chamber is isolated from the pump, the pressure of which starts to rise due to air flowing from the concrete pores (at atmospheric pressure) into the vacuum cell. The pump goes on working on the outer chamber at a speed controlled by a pressure regulator, in order to keep the pressure of both chambers balanced. Under these conditions, it can be assumed that air flows into the central

chamber unidirectionally (a cylinder of air), whilst the lateral flow is sucked by the external chamber that acts as a guarding. Applying a physical model, it is possible to compute the coefficient of air-permeability of concrete  $kT$  from the data recorded during the test: atmospheric pressure Pa, ‘effective’ pressure rise in the inner chamber  $\Delta P$  between  $t_0 = 60$  s and  $t_f =$  time at the end of the test ( $\leq 720$  s). The model provides also an estimate of the penetration of the vacuum front  $L$ , affected by the test. A derivation of the formula to compute  $kT$  and  $L$  can be found in (Torrent et al, 2022; M-A-S, 2023).

The instrument used for the experiments was the 5<sup>th</sup> Generation PermeaTORR AC+ (M-A-S, 2023), that allows to monitor the pressure rise in the inner chamber with time.

The test was applied, first on the unloaded specimens, obtaining the reference permeability. This was done on two faces of all 17 cubes.

Cubes #3, 4 and 5 were loaded to a stress of 13.5 MPa (30% of  $f'_{cm}$ ). Once the desired level of stress was attained, the load was kept constant during a time sufficient to perform two  $kT$  test, on two opposite faces (A and B) of each cube. Then the cube was unloaded and removed from the testing machine.

Cubes #8, 9 and 10 followed the same procedure, only that the level of stress was raised to 27.0 MPa (60% of  $f'_{cm}$ ). Finally, cubes #11 and 12 were similarly tested at a stress level of 40.5 MPa (90% of  $f'_{cm}$ ).

Immediately afterwards, all eight cubes mentioned above were tested again for  $kT$ , now without any applied load, obtaining

Face	1A	2A	3A	4A	5A	6A	7A	8A	9A
$kT$ ( $10^{-16}$ m <sup>2</sup> )	0.0661	0.0177	0.0249	0.0208	0.0376	0.0359	0.0271	0.0479	0.0270
Face	10A	11A	12A	13A	14A	15A	16A	17A	
$kT$ ( $10^{-16}$ m <sup>2</sup> )	0.0214	0.0358	0.0127	0.0263	0.0263	0.0293	0.0293	0.0301	
Face	1B	2B	3B	4B	5B	6B	7B	8B	9B
$kT$ ( $10^{-16}$ m <sup>2</sup> )	0.0529	0.0412	0.0183	0.0385	0.031	0.0376	0.0489	0.0605	0.0159
Face	10B	11B	12B	13B	14B	15B	16B	17B	18B
$kT$ ( $10^{-16}$ m <sup>2</sup> )	0.0263	0.0309	0.0325	0.0270	0.0183	0.0420	0.0341	0.0256	

**Table 2:** Results of  $kT$  obtained on two faces of the 17 unloaded reference cubes

It is worth mentioning that the penetration of the test  $L$ , described above, ranged between 10 and 20 mm, depending on the measured value of  $kT$ .

### Sustained Load and “Residual” $kT$ values

The values of  $kT$  measured under sustained loads (‘Loaded’) and after removal of the load (‘Residual’) are shown in Table 3 for the three levels of stress applied. For comparison, the corresponding unloaded values (taken from Table 2) are also indicated. It was not possible to get meaningful values of  $kT$  on some of the cubes subjected to 40.0 MPa compressive stress.

the so-called “Residual” air-permeability  $kT$ .

Cubes #1, 2, 7, 14 and 15 were placed in the testing machine, applying a compressive stress that increased monotonically at a predefined rate until failure. The pressure rise in the inner chamber  $\Delta P$  was monitored continuously during the entire test with the PermeaTORR AC+ instrument. Only one face of each cube was monitored.

For reasons that will be explained later, cubes #3 and 4, that had been loaded up to 13.5 MPa and unloaded afterwards, were saw-cut into two halves, each cube producing two prisms of 70×150×150 mm. These prisms were also loaded monotonically as explained in the previous paragraph until failure, whilst monitoring the pressure rise in the inner chamber  $\Delta P$ .

1. The ‘effective’ pressure rise is the difference between the pressure rise recorded during a test and that recorded during the calibration of the instrument at the same time, when applied on an impermeable plate.

### Test Results

#### Reference unloaded Air-Permeability $kT$

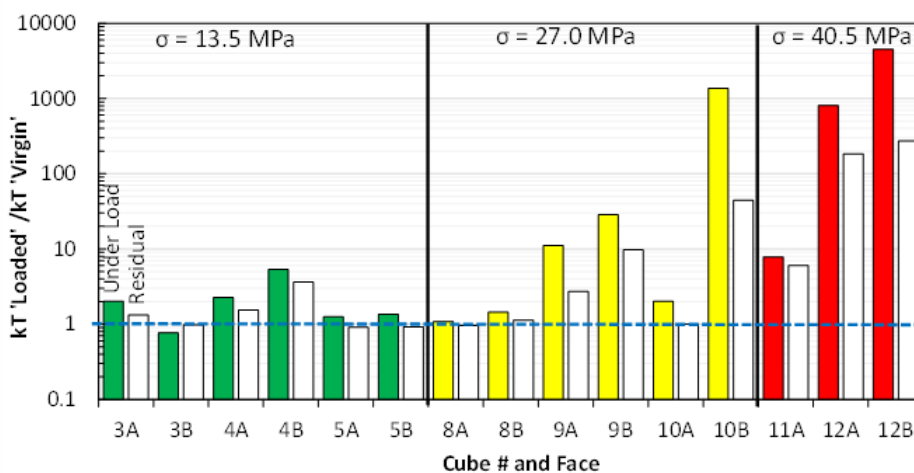
The 34 test results obtained on two faces of the 17 cubes investigated are presented in Table 2. The uniformity of the results is excellent, with all values belonging to the ‘Low’ Permeability Class ( $0.01 \times 10^{-16} \text{ m}^2 < kT < 0.1 \times 10^{-16} \text{ m}^2$ ). The geometric mean of the results is  $kT_{gm} = 0.0301 \times 10^{-16} \text{ m}^2$  and the standard deviation of the decimal logarithms of the results is  $sLOG = 0.163$ .

<i>kT</i> values ( $10^{-16}$ m <sup>2</sup> ) measured for Sustained Applied Stress of											
13.5 MPa				27.0 MPa				40.0 MPa			
Face	Virgin	Loaded	Residual	Face	Virgin	Loaded	Residual	Face	Virgin	Loaded	Residual
3A	0.0249	0.0499	0.0328	8A	0.0479	0.0520	0.0460	11A	0.0358	0.280	0.215
3B	0.0183	0.0140	0.0180	8B	0.0605	0.0874	0.0685	11B	-	-	-
4A	0.0208	0.0470	0.0320	9A	0.0270	0.2996	0.0733	12A	0.0127	10.3	2.34
4B	0.0385	0.2057	0.1396	9B	0.0159	0.4534	0.1542	12B	0.0325	146.0	8.89
5A	0.0376	0.0469	0.0342	10A	0.0214	0.0431	0.0215	13A	-	-	-
5B	0.0310	0.0421	0.0287	10B	0.0263	35.9	1.16	13B	-	-	-
Median of Ratios	1.68	1.15		Median of Ratios	6.56	1.92		Median of Ratios	808	184	

**Table 3 :** Results of *kT* obtained on cubes subjected to sustained loads of different levels

In the last row of Table 3, the median of the ratios of *kT* Loaded/unloaded and Residual/ unloaded are indicated for each load level. The median is used to cushion the high scatter recorded at high levels of load. It can be seen that the application of load, even of just 30% of the compressive strength, increases the *kT* air-permeability, although the removal of the load brings the values very close to the unloaded values. These results are at odds with those reported earlier (Paulík & Hudoba, 2009; Van der Merwe, 2019), in which no-change of *kT* permeability was found at loads  $\leq$  50% of the compressive strength. One possible interpretation of the results reported in Table 3 is that, at 30% level of load, micro cracking at the interface paste-aggregate occur, which is enough to increase the air-permeability *kT*. The removal of the load closes these micro cracks, returning the *kT* values close to the unloaded ones. At higher levels of loading, especially at the 90% level, both the *kT* values under load and after unloading become much higher than the original ones, reflecting the more severe cracking experienced by the specimens.

The results shown in Table 3 are presented graphically in Fig. 2. The ratio of the *kT* results obtained under sustained load (coloured bars) and after removing the load, i.e. ‘Residual’ (white bars), referred to the *kT* values obtained on the unloaded specimens, are displayed for each cube. The results under sustained load are painted in green, yellow and red for applied loads of 13.5, 27.0 and 40.5 MPa, respectively.



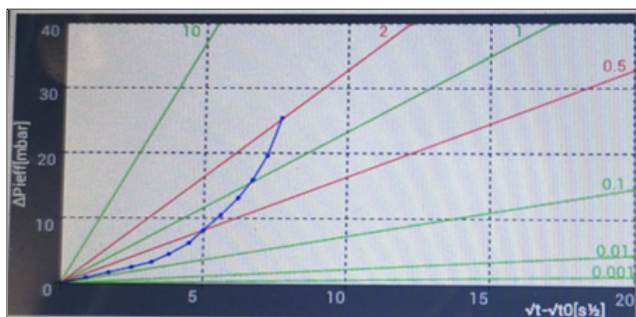
**Figure 2:** Relation between the permeability *kT* measured on loaded specimens referred to the unloaded values

Fig. 2 shows that at a relatively low level of stress (13.5 MPa;  $\approx$  30% of the strength) a slight increase in air-permeability – under sustained load - is already detectable in five out of the six faces investigated. The same five faces showed a recovery of the *kT* value after removal of the load (‘Residual’ values), such that in three out of the six samples the ‘Residual’ value returned to the original unloaded value. This indicates that the damage inflicted under load, was possibly due to interface micro cracks that were closed after the removal of the load.

For higher levels of stress, the departure of the ‘Loaded’ *kT* values from those measured on the unloaded specimens becomes larger reaching, for certain samples values that are 3 orders of magnitude higher than those of the unloaded specimens. With a couple of exceptions, the ‘Residual’ *kT* values are higher than those measured on the unloaded samples reaching *kT* ratios 2 orders of magnitude higher. This indicates that a permanent damage has been inflicted to the specimens loaded at 60 and 90% of the compressive strength.

### ***kT* Under Monotonically Increasing Load**

In this kind of test, instead of referring to the *kT* result, the focus will be placed on the relation between  $\Delta P$  and the square root of the time ( $\sqrt{t} - \sqrt{t_0}$ ) which, according to the model should be linear if the porosity, permeability, moisture and temperature are constant within the volume of material affected by the test (Torrent et al, 2022; M-A-S, 2023). The plot is automatically displayed by the *PermeaTORR AC+* instrument during the test, as shown in Fig. 3a for the test under monotonically increasing load on face B of cube #1, in which a clear non-linearity is visible. The departure from linearity can be attributed to the creation and propagation of cracks during the loading. On the other hand, Fig. 3b shows the plot corresponding to face A of cube #2, under the same type of loading, which remains quite linear.



**Figure 3a:** Non-linear relation between  $\Delta P$  and  $(\sqrt{t} - \sqrt{t_0})$  for Cube #1 under monotonical loading

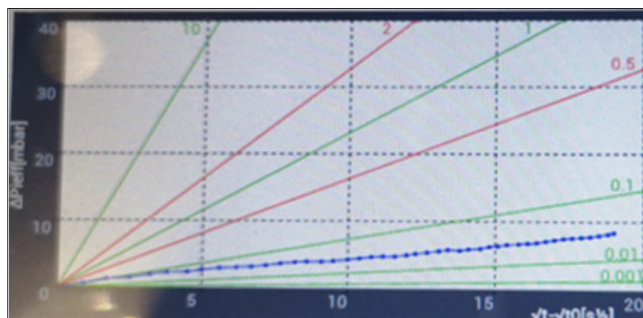


**Figure 3b:** Quasi-linear relation between  $\Delta P$  and  $(\sqrt{t} - \sqrt{t_0})$  for Cube #2 under monotonical loading

The interpretation of the quasi-linear plot in Fig. 3b is that, given that the penetration of the test for the unloaded cubes is less than 20 mm, by chance the damage may happen in areas of the cube outside the reach of the permeability test, which showed a quasi-linear relation, similar to that obtained when testing an unloaded sample.

In order to overcome this problem, an attempt was made to saw-cut in halves cubes #3 and 4, previously subjected to a load of 13.5 MPa (with little damage), as described in Section 2.2. Now, with a thickness of the tested element reduced from 150 to 70 mm, the chance that the *kT*-test is affected by the cracks created during the monotonic loading is increased.

The data of  $\Delta P$  as function of the time *t* are stored in the memory of the instrument, which allows to reproduce the plot  $\Delta P$  vs  $(\sqrt{t} - \sqrt{t_0})$  numerically.

The term Unloaded is expressed within inverted commas, because these samples had been previously subjected to a load of 13.5 MPa.

Fig. 4 shows, for face A of half-cube #3, the plot  $\Delta P$  vs  $(\sqrt{t} - \sqrt{t_0})$  for the ‘Unloaded’ sample (continuous black line) and for the permeability test conducted, while the specimen was subjected to a monotonic load at a rate of 0.2 MPa/s (red line with red circles). The blue dotted line with crosses represents the difference between the  $\Delta P$  measured on the specimen under load and that measured on the unloaded specimen, represented as  $\Delta\Delta P$ .

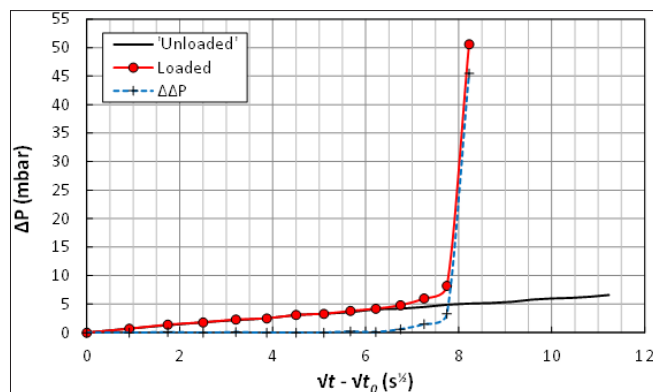


**Figure 4:** shows, for face A of half-cube #3, the plot  $\Delta P$  vs  $(\sqrt{t} - \sqrt{t_0})$  for the ‘Unloaded’

The plot of  $\Delta\Delta P$  indicates that the specimen experiences a visible increase in its permeability at  $\sqrt{t} - \sqrt{t_0} \approx 6.25$  s<sup>1/2</sup> or, recalculating, at a time  $t \approx 195$  s since the initiation of the *kT*-test. As the testing machine applies the load at a prescribed rate, taking one or two reference readings, it is possible to convert the time scale into a stress scale.

Fig. 5 presents the data of  $\Delta P$  of three loaded half-cubes and the corresponding  $\Delta\Delta P$  values, as function of the applied stress/compressive strength ratio ( $\sigma/f^c$ ). It has to be mentioned that the instrument automatically stops the test once the value of  $\Delta P$  has exceeded 20 mbar (horizontal black line).

The three specimens show quite different behaviours in terms of the level of stress at which the loaded sample starts to show an increase in permeability compared to the same specimen tested ‘unloaded’. Indeed, half-cube 4B departs at a  $\sigma/f^c$  ratio as low as 15%; the same departure happens at  $\sigma/f^c$  ratios of 46% and 70% for half-cubes 4A and 3A, respectively.

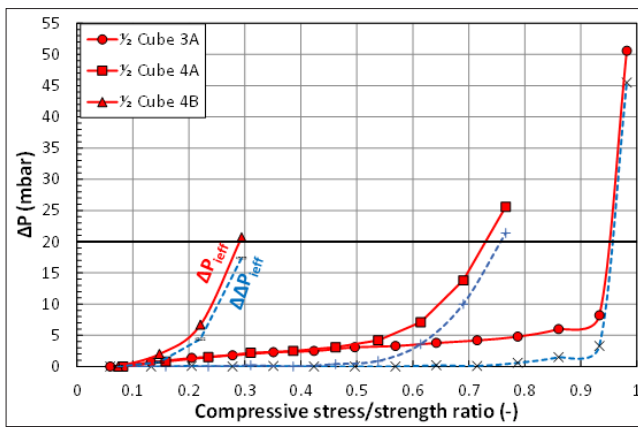


**Figure 5:** Relation between  $\Delta P$  and  $\Delta\Delta P$  with  $\sigma/f'c$  ratio for the three half-cubes tested

The permeabilities measured at the end of the tests resulted of 7.3, 3.3 and 13.2 ( $\times 10^{-16}$  m<sup>2</sup>) for half-cubes 3A, 4A and 4B, respectively. It is interesting to note that face B of cube #4 had shown a high permeability, both under sustained loaded at 13.5 MPa and after removal of the load (see Table 3), which may suggest that the corresponding half-cube had already some damage before starting the test under monotonical loading.

### Conclusions

The results obtained in this investigation allow us to draw the following conclusions:

1. Contrary to previous investigations, the tests made under sustained load at a level of 30% of the compressive strength showed a slight increase in  $kT$  permeability compared to that of the unloaded specimens, that almost disappeared when the load was removed. This may be attributed to interface micro cracks that close after unloading.
2. The increase of  $kT$  at that level of stress is, in average, around 70%. Taking into consideration that  $kT$  varies, as function of the quality of the concrete, over six orders of magnitude (Torrent et al, 2022; M-A-S, 2023), this increase is not significant in practical terms.
3. At load levels of 60% and 90% of the compressive strength, the increase in  $kT$ , measured under load and after the removal of the load, became more marked indicating more severe cracking that remained open after unloading. In the case of 90% loading, the increase in  $kT$  under load reached three orders of magnitude for measurements under load and two orders of magnitude for measurements after removal of the load, respect to that of the unloaded specimens.
4. The measurement of  $kT$  under monotonic compressive loads looks promising; yet, the random location of the damage sometimes eludes the reach of the air-permeability test, giving erratic values. Preliminary tests, on previously loaded cubes saw-cut in halves, suggest that, measuring  $kT$  on both faces of 70×150×150 mm prisms may lead to more accurate and homogeneous results.

### References

1. Hsu, T.T.C., Slate, F.O., Sturman, G.M. & Winter, G. (1963). Microcracking of plain concrete and the shape of the stress-strain curve. *J. ACI Proc.*, 60(2), 209-224. Retrieved from <https://www.semanticscholar.org/paper/Microcracking-of-Plain-Concrete-and-the-Shape-of-Hsu-Slate/5939abf6ab5d9591acdeef8c8ad487d86d509ce9>
2. Shah, S.P. & Slate, F.O. (1968). Internal microcracking, mortar-aggregate bond and the stress-strain curve of concrete. *Cem. & Concr. Assoc., London, UK*, 82-92. Retrieved from <https://www.semanticscholar.org/paper/INTERNAL-MICROCRACKING%2C-MORTAR-AGGREGATE-BOND-AND-Shah-Slate/650dff669e23df32fcd677c39a691764406ef3e>
3. Newman, K. & Newman, J. B. (1971). Failure theories and design criteria for plain concrete. Proc. Southampton 1969 Civil Eng. *Materials Conf.* (M. Te'eni Ed.), John Wiley & Sons, Bristol, UK, Part 2, 963-995.
4. Rusch, H. (1960). Researches towards a general flexure theory for structural concrete. *Zement-Kalk-Gips*, 12, 1-9. Retrieved from <https://www.semanticscholar.org/paper/Researches-Toward-a-General-Flexural-Theory-for-Rusch/f62deb8b1529fdf2c2c10ea30d1f0374409eefd4>
5. Dantu, P. (1958). Study of the stresses in non-homogeneous materials and its application to concrete. *Ann. l'Inst. Techn. Bat. Trav. Publ.*, 11, 55-77.
6. Mlakar, P.F., Walker, R.E., Sullivan, B.R. & Chiarito, V.P. (1984). *Acoustic Emission Behavior of Concrete*. ACI SP-82, 619-637.
7. Hoseini, M., Bindiganavile, V. & Banthia, N. (2009). The effect of mechanical stress on permeability of concrete: A review. *Cem. & Concr. Composites*, 31(4), 213–220. DOI: <http://dx.doi.org/10.1016/j.cemconcomp.2009.02.003>
8. Torrent, R., Neves, R. & Imamoto, K. (2022). "Concrete Permeability and Durability Performance – From Theory to Field Applications". *CRC Press*, Boca Raton, FL, USA and Abingdon, Oxon, UK, 570 p.
9. Meziani, H. & Skoczylas, F. (1999). An experimental study of the mechanical behaviour of a mortar and of its permeability under deviatoric loading. *Mater. & Struct.*, 32, 403–409. Retrieved from <https://link.springer.com/article/10.1007/BF02482711>
10. Banthia, N. & Barghava, A. (2007). Permeability of stressed concrete and role of fiber reinforcement. *ACI Materials Journal*, 104(1), 70–77. Retrieved from [https://www.researchgate.net/publication/279908560\\_Permeability\\_of\\_stressed\\_concrete\\_and\\_role\\_of\\_fiber\\_reinforcement](https://www.researchgate.net/publication/279908560_Permeability_of_stressed_concrete_and_role_of_fiber_reinforcement)
11. SIA 262/1 (2019). "Construction en béton . Spécifications complémentaires, Swiss Standard, 1 March 2019, 60 p. (in French and German).
12. NDIS 3436-2 (2020). Non-destructive testing of concrete - Air permeability testing method Part 2: Double chamber method. *Japan Soc. Non-destructive Inspection (JSNDI)*, 15 p. (in Japanese).

- 
13. IRAM 1892 (2022). Hormigón. Método de ensayo para la determinación del coeficiente de permeabilidad al aire (kT) del hormigón endurecido. *Argentine Standard* (in Spanish).
  14. Paulík, P. & Hudoba, I. (2009). The influence of the amount of fibre reinforcement on the air-permeability of high performance concrete. *Slovak J. Civil Eng.*, 2, 1–7. Retrieved from [https://www.svf.stuba.sk/buxus/docs/sjce/2009/2009\\_2/file4.pdf](https://www.svf.stuba.sk/buxus/docs/sjce/2009/2009_2/file4.pdf)
  15. Van der Merwe, J. (2019). “Constitutive models towards the assessment of concrete spalling in fire”. PhD Diss. ETH No. 26205, ETHZ, Zürich, 235 p.
  16. M-A-S (2023). Materials Advanced Services Ltd. Retrieved from [www.m-a-s.com.ar](http://www.m-a-s.com.ar).

**Copyright:** ©2023 Torrent R. This is an open-access article distributed under the terms of the Creative Commons Attribution License, which permits unrestricted use, distribution, and reproduction in any medium, provided the original author and source are credited.